

# Development of an Indexing Media Filtration System for Long Duration Space Missions

Juan H. Agui\*

*NASA Glenn Research Center, Cleveland, OH, 44135*

*and*

R. Vijayakumar†

*Aerfil, Liverpool, NY, 13088*

The effective maintenance of air quality aboard spacecraft cabins will be vital to future human exploration missions. A key component will be the air cleaning filtration system which will need to remove a broad size range of particles including skin flakes, hair and clothing fibers, other biological matter, and particulate matter derived from material and equipment wear. In addition, during surface missions any extraterrestrial planetary dust, including dust generated by near-by ISRU equipment, which is tracked into the habitat will also need to be managed by the filtration system inside the pressurized habitat compartments. An indexing media filter system is being developed to meet the demand for long-duration missions that will result in dramatic increases in filter service life and loading capacity, and will require minimal crew involvement. These features may also benefit other closed systems, such as submarines, and remote location terrestrial installations where servicing and replacement of filter units is not practical. The filtration system consists of three stages: an inertial impactor stage, an indexing media stage, and a high-efficiency filter stage, packaged in a stacked modular cartridge configuration. Each stage will target a specific range of particle sizes that optimize the filtration and regeneration performance of the system. An 1/8<sup>th</sup> scale and full-scale prototype of the filter system have been fabricated and have been tested in the laboratory and reduced gravity environments that simulate conditions on spacecrafts, landers and habitats. Results from recent laboratory and reduce-gravity flight tests data will be presented.

## Nomenclature

$A$	=	filter element cross-sectional area
$C_c$	=	slip coefficient
$d_{50}$	=	particle diameter at 50% efficiency
$D_J$	=	jet diameter
$K_p$	=	medium permeability
$Q$	=	flow rate
$Re$	=	Reynolds number
$U$	=	jet velocity
$Stk_{50}$	=	Stokes number at $d_{50}$
$w$	=	width of impactor band
$\rho_p$	=	particle density
$\mu$	=	viscosity
$\tau$	=	relaxation time

---

\* Aerospace Engineer, Fluid Physics and Transport Branch, 21000 Brookpark Rd, Mail Stop 77-5, Cleveland, OH, AIAA Member .

† President

## I. Introduction

In order to provide safe and sustainable breathable air aboard crewed space vehicles and extraterrestrial outposts, effective dust mitigation techniques are needed for remote and long duration space operation. Filtration systems are a vital component of life support systems removing nuisance and harmful particulates that ultimately provide clean air and comfort for human health. However, filtering of airborne particles under the environmental constraints and conditions of spacecraft and planetary surface system poses unique challenges. The filter system not only must be capable of removing fine particles such as skin flakes, hair and clothing fibers, and particulate matter from food and hygiene operations, it also needs to remove debris from operating machinery, equipment, and science payloads and planetary dust tracked in by extravehicular activity (EVA). Thus the system must be capable of filtering particles sizes spread over several orders of magnitude. Further, since servicing or replacing filters in space is not a trivial task, the system is also required to last extraordinary life times.

Filtration technologies are well established in terrestrial applications. However, they rely on replacement units for continued operation. On long duration crewed space missions this practice may not be very feasible. Specifically high efficiency fibrous filters, which make up the bulk of filter elements on air handling systems, are excellent at providing greater than 99.9% particle capturing efficiency, but are virtually impossible to regenerate without damage to the filter media. This is because dust particles adhere tenaciously to the fibers throughout the depth of the filter. However, HEPA (High Efficiency Particulate Air) filters for example if properly pre-filtered can have service lives in excess of 5 years with some cleanroom filters lasting for over 25.<sup>‡</sup> Therefore it is proposed that regeneration needs to be accommodated through alternate filtration or separation means in conjunction with high efficiency filtration. This paper describes a novel multi-stage filter system that has been designed under an Innovative Partnership Program (IPP) project between NASA and Aerfil. Prototypes of the Indexing Media Filtration system (also known as the scroll filter) have been developed. The filter system is designed to meet the demand for long-duration missions by providing dramatic increases in filter service life and loading capacity, and will require minimal crew involvement. The filtration system consists of three stages: an inertial impactor stage, an indexing media stage, and a high-efficiency filter stage, packaged in a stacked modular cartridge configuration. Each stage targets a specific range of particle sizes that optimize the filtration and regeneration performance of the system. This modular design also provides the flexibility to add more stages of filters for performance optimization, and to meet design and operational requirements of any NASA mission.

## II. Hardware Description

### A. The filter system

Two different scale prototypes of the scroll filter system were designed and fabricated, and subsequently tested under laboratory and low-g conditions. First, a reduced-scaled (approximately 1/8-th scale, based on the ratio of cross-sectional areas) prototype, 10.8 cm x 10.8 cm in cross-section, of the indexing media filtration system was fabricated through stereolithography (SLA)-based rapid-prototyping. The filtration system consisted of three stages: an inertial impactor stage, an indexing media stage, and a high-efficiency filter stage, packaged in a stacked modular cartridge configuration. Subsequently, a full scale prototype of the scroll filter was fabricated through an international partner (contracted through Aerfil). The prototype system has the same staged design as the scaled prototype. It has a cross-sectional area of 30 cm x 30 cm and was built structurally from aluminum sheet metal. Both prototypes were designed to be flexible to accommodate different performance characteristic filter elements. They were designed to operate at a nominal 0.047 m<sup>3</sup>/s (100 cfm, full scale performance) and 0.0057 m<sup>3</sup>/s (12 cfm) of atmospheric air for the full scale and 1/8-th scale prototypes respectively. The equivalent face velocity encountering the filter elements is 0.5 m/s which is a nominal velocity for high efficiency filters in terrestrial use. A picture of the full scale prototype is provided in Figure 1. It consists of several in-line, stacked, stages. The entrance duct serves for testing purpose to properly filter and develop the incoming flow, as well as to introduce the challenge aerosols for filter testing. The impactor and scroll stages are the actual filter elements that are tested. And the conic end section is for interfacing with the air suction source, which could be provided through a blower, fan, or vacuum system. The windows provide a means of observation and optical access for flow diagnostics. The picture to the right shows a comparison between the full scale and reduced scale prototypes.

---

<sup>‡</sup> Based on the second author's more than 25 years of experience in the industry.

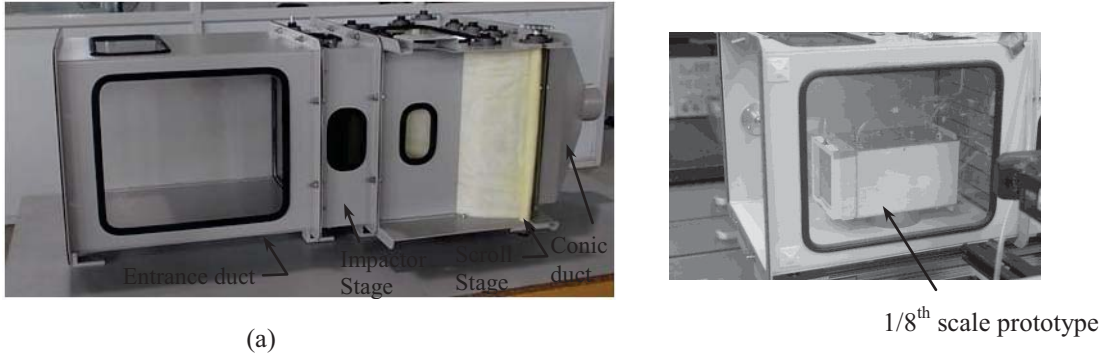


**Figure 1: (a) full scale Indexing Media Filter System, (b) full and reduced-scale prototypes (scale model placed inside full scale model for size comparison).**

The multi-stage air filtration system utilizes an inertial impactor filter stage, an indexing media filter and a HEPA filter in a series configuration. The HEPA filter was not installed in the picture of the filter system in Figure 1. The purpose of the inertial filter stage is to capture the largest particulates in order to reduce loading of the indexing media filter and/or (depending on configuration) HEPA filter stages, thereby prolonging the filter system's service life. The indexing media filter, or scroll stage, captures intermediate particle sizes (typically a few microns). Since this filter stage is expected to become heavily loaded with particulate matter over long operations, or due to high loading events, it must be regenerated or replenished by dust mitigation means involving very low-maintenance components. To minimize maintenance, the indexing media filter will be replenished by means of a motorized spool that rolls up the dust laden portion of the filter media on one side of the filter housing, thereby removing the accumulated dust and replenishing the dust-laden filter section with fresh media. The HEPA filter is the last stage of filtration and therefore its role is to capture the remaining (smallest) particulates with very high efficiency. The HEPA stage was not installed for testing since HEPA air filter performance is well characterized throughout the industry.

The principle of the impaction or impingement stage is that particles are collected on bluff flat surfaces normal to the flow. A conceptual schematic of the flow and particle trajectories is shown in Figure 2. The flow is accelerated through the orifice aperture on the plate and then is suddenly redirected near the flat surface of the plate or strip directly behind the orifice. The high turning angle causes relatively large particles to impact the plate while the smaller particles, which are well entrained in the flow, pass by the plate surface and continue downstream with the flow. Equation 1 provides a relationship between the  $d_{50}$  cut size, i.e. the diameter of particles at which 50% of particles get collected on the impactor plate, and other design and flow variables. This equation shows the relationship among the  $d_{50}$  cut size, the impactor geometry, and the particle transport (Stokes number) and flow (Reynolds number) parameters (see Ref. 1).

$$d_{50} = \sqrt{\frac{9D_j^2 Stk_{50}}{C_c \rho_p Re}} \quad (1)$$

Where  $D_j$  is the jet diameter,  $C_c$  is the Cunningham Slip Correction factor,  $\rho_p$  is the particle density, and  $Stk_{50}$  and  $Re$  are the Stokes number for the  $d_{50}$  particle diameter and Reynolds number defined as,

$$Stk_{50} = \frac{\tau U}{(D_j / 2)} \quad (2)$$

$$Re = \frac{UD_j}{\mu} \quad (3)$$

The variable  $\tau$  is the relaxation time which is the time needed by the particle to adjust, or relax, to changes in flow conditions, defined as,

$$\tau = \frac{\rho_p d^2 C_c}{18\mu} \quad (4)$$

and  $\mu$  is the fluid viscosity.

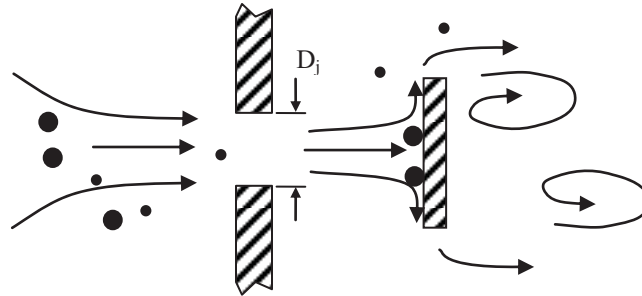


Figure 2: Flow schematic through an inertial impactor

Based on these equations, the orifice or nozzle jet diameter is chosen based on the  $d_{50}$  particle filtration requirement and flow conditions. Alternately the  $d_{50}$  can be set by the controlling the jet velocity, which appears in the Reynolds number. This permits designs with other than circular orifice geometries. The performance of the impactor is not very sensitive to the width of the collection strip or the separation distance between the orifice and collection strip. The hardware or system constraints and requirements can dictate these dimensions, while the width of the strip needs to be at least slightly wider than  $D_j$ . In the scale prototype, the orifice openings consisted 4 sets of approximately two hundred 1 mm diameter straight hole perforations in a long rectangular raster pattern that were micro-machined on a thin 1.5 mm thick orifice plate. Alternately, because of the challenge of scaling up this type of fabrication and to minimize air resistance the orifice openings on the full scale prototype consisted of eight 3 mm wide slots machined on the orifice plate. A nominal  $d_{50}$  of  $5\mu\text{m}$  was selected for the current filter designs.

The impactor stage incorporates endless bands or belts that span across most of the width of the duct just behind (downstream) of the orifice plate. A thin layer of grease on the surface of the belt facing the incoming flow minimizes particle rebound and facilitates their cleaning. The belts ride on pulleys mounted on vertical spindles placed internally near the inside of the duct side walls. The user has access to the tops of the spindles that extend above the top wall and can manually rotate the spindles. As one of the spindles is rotated from above the belts are translated across the width of the duct and eventually cycle all the way around the belt loop. In the full scale prototype the belts encounters a wiper or scraper that removes the layer of particles and grease as they cycle through the loop.

The scroll media stage provides excess filter media that is supplied and collected on spools. A servo motor is activated to start scrolling the media and exposing a fresh surface of the medium to the flow. The filter medium is threaded through a series of internal spindles that allow the medium to form pleats inside the duct. Pleats are very beneficial in air filtration because they increase the filter surface area and reduce the media velocity, both aspects leading to better filter performance. All internal spindles and outer spools are mounted on roller bearings to facilitate the spooling operation and reduce the motor power requirements. The design of the system allows for installation of any grade of filter media to meet the desired filtration specification of the scroll filter. In the prototypes tested, commercial grades of filter media with performance in the MERV (Minimum efficiency reporting value) 11 to 15 range, typically used to capture particulates from  $0.3\mu\text{m}$  to  $1.0\mu\text{m}$ , were installed on the scroll filter stage. Fibrous filter media is used ubiquitously in air filtration because it is cost-effective and also provides an effective method of filtration known as depth filtration. Figure 3 shows a typical filtration performance curve for depth filters. Depth

filters can capture most particles sizes that pass through it with virtually 100% efficiency, while a portion of the particles in the narrow band between 0.03 and 0.5  $\mu\text{m}$ , typically, can penetrate through. This is due to a less than complementary transition from the diffusional mode of filtration (at the smallest particles sizes) to the inertial mode of filtration (at the largest particle sizes), that permits a small amount of particle penetration in this size range. These effects are represented in Figure 3. However, despite the success and practicality of depths filters in terrestrial applications, depths filters are highly susceptible to caking and fouling which drives up their air resistance and in turn requires more system power to continue in operation until the filter is changed. The scroll filter is in effect a self-changing or self-cleaning filter system where the filter medium is autonomously (or through user control) replaced.

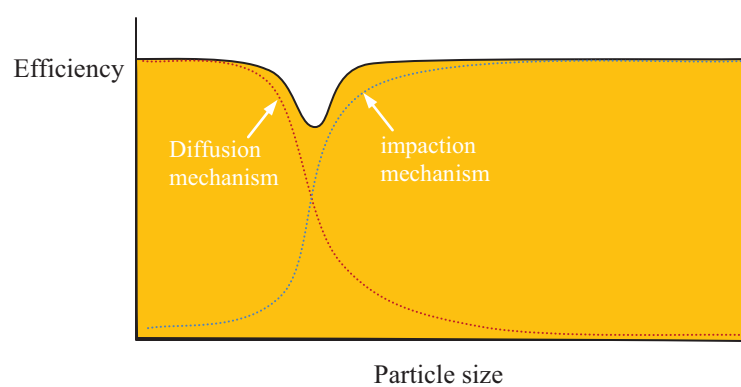


**Figure 3: Typical capturing efficiency curve for a depth filter showing the contribution to efficiency from the diffusional and inertial impaction capturing mechanisms.**

## B. Testing platform

The prototypes were assembled and tested on a portable test rig which was used in the laboratory setting as well as installed on the Zero-g aircraft for low gravity testing. A picture of the test rig configured for flight appears in Figure 4. The experimental rig was designed as a multi-use test stand to assess the performance of filter systems and components. The scaled prototype was tested first and was internally mounted to an existing duct assembly from a previous flight experiment. Therefore, the flow had to internally transition between the larger duct dimensions to the that of the scaled prototype. The flow was driven by a bank of four axial fans in a square configuration at the end of the duct length. Alternately, no flow transition section was required in the entrance region of the full scale prototype because the ducting of the filter system itself was used to interface directly to the flow source. The flow was driven by a high capacity commercial HEPA vacuum cleaner that suctioned the flow through the entrance duct and filter stages. The vacuum cleaner inlet interfaced with the ducted sections through a transition conic section shown in Figure 1. The bottom shelf of the test rig provides most of the power and signal avionics required for testing. Measurements of pressure drops across filter elements, entrance duct flow speeds, particle counts and sizes, and imaging of the particle flow were conducted on the rig. Pressures measurements were performed with low pressure differential pressure transducers. Flow velocities were measured in clean air, before particles were introduced in the flow, using hot-wire based velocity probes supplied by Dantec Dynamics.<sup>§</sup> A pair of Lighthouse 3016 particle monitors were used to simultaneously measure the particle counts upstream and downstream of the filter elements. These units permit simultaneous measurement of six channels of particle sizes from 0.3 to 10 microns. The data were logged through a USB National Instruments Data Acquisition device and run through Labview Software. Samples were taken at 1 kHz sampling rate for 10 seconds to average out any transients. One Sony HD camcorder along with a superbright LED light source and some optical components were used to image the particle flow in the upstream region as well as image the indexing/scrolling operations.

A custom designed particle generator initially designed for close-system operation was used in all tests. A description of the particle generator is provided in Ref. 2. It provides sustained solid particle injections without introducing additional air flow into the system. Since it produces a wake flow, instead of a jet flow as with some commercial particle injectors, it can produce faster spreading and mixing of the particles as they advect downstream.

<sup>§</sup> NASA does not specifically endorse any vendor's products.

While the particle generator performed well in both sets of tests, it was found by subsequent analysis that the shorter distance between the particle generator and the first (upstream) sampling probe in the scale prototype case most likely did not allow for sufficient particle dispersion at this measuring station. As a consequence the upstream particle counts were considered to be significantly skewed to larger values. This issue is discussed later in the results section.

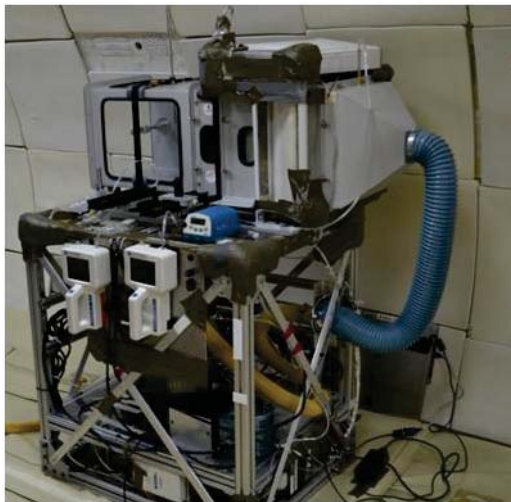


Figure 4: Test rig with full scale prototype installed in the Zero-G aircraft.

### III. Materials and Methods

The objective of this investigation was to conduct a characterization of the overall performance of the new filtration system.

Methods for testing conventional filters, such as the filter media used in the current set of tests, are fairly standard. In the industry, these methods rely on well established, often large, testing facilities that provide uniform air and particulate flows. Similar methods will be applied to the new filter system, noting however that under the current test plan testing was confined to a smaller footprint testing platform and that it involved the testing of certain non-conventional, non-media, components. Also to achieve relevant space related conditions, alternate approaches to particle exposure methods were also taken.

The two main performance parameters that describe filter functionality is permeability and collection efficiency. High permeability coupled with high particle capturing efficiency is a desirable characteristic of high efficiency filtration. These parameters are typically determined by subjecting a flat sheet of filter media to well controlled flow conditions and challenging it with aerosol standards (see ASHRAE<sup>3</sup>, IEST<sup>4</sup>, ISO 29463<sup>5</sup> test standards). In these test protocols the pressure drop across the filter element, and particle counts in the flow upstream and downstream of the filter element are used in the calculation of the performance parameters. However, since our interest is in the overall performance of the filter system under relevant space related conditions, certain variations of the standard test protocol were adapted. First, the filter system was tested in the customized test rig described in the previous section which constrained some of the testing techniques. An additional level of flow characterization was required of the impaction collection device which was expected to significantly alter the flow in the surrounding flow field. The hydrodynamic performance of the impactor stage was characterized by its performance (or resistance) curves, pressure vs. flow rate. This characterization is relevant because it relates to the level of power usage to drive the flow. To account for the scroll filter's pleated configuration, permeability for the scroll media is given in terms of the flow rate per unit area at a specified pressure drop, i.e.  $K = Q/A$  at a prescribe  $\Delta P$ . Lastly, because of the interest in testing under relevant environmental conditions, a lunar dust simulant was used instead of using particle standards.

Filter efficiency, or particle collection efficiency, was determined from the ratio of particle counts upstream and downstream of the filter element. The challenge aerosols used in this case, were derived from JSC-1af lunar dust simulant and JSC-Mars-1 equivalent simulants. JSC-1af is a basaltic based mineral powder with 20 wt % of the particles below 10  $\mu\text{m}$  in size.<sup>6</sup> The Martian simulant is an equivalent JSC-Mars 1 simulant derived from palagonite mineral from Mauna Kea, Hawaii. These simulants have an average density of 2.9  $\text{g}/\text{cm}^3$  which tends to make them settle relatively quickly during testing. To mitigate this, the entrance region where the particles are introduced is made shorter than standard entrance or development regions for filter testing, that typically require an entrance length of at least 10 characteristic duct lengths. The shorter entrance length however can reduce the mixing and spreading of the aerosols needed for proper testing prior to the measuring stations. The other mitigating approach is to test in low or micro-gravity conditions which can reduce or eliminate particle settling. Although this helps with minimizing settling, the dispersion of the particles prior to reaching the first filter stage is still constrained by the shorter entrance length. In fact the length of the entrance duct was kept short in anticipation of low-g testing, in which often there is a benefit in containing the overall size of the flight payload for manifesting purposes.

Limited low-g testing of both prototypes were performed on the Zero-G Corporation aircraft through NASA's Flight Opportunities Program. The aircraft performs parabolic arc maneuvers that transition between low-g levels (zero to planetary surface gravity levels) to high-g (approximately 1.8 earth g's) levels. Multiple simulated low-g gravity periods are performed during a typical flight, which provides the researchers about 20 seconds periods of steady low-g levels for testing their hardware.

Table 1 provides a list of test configurations presented in the results section.

**Table 1: Filter test configuration**

Configuration	Prototype	Impactor	Scroll Media	Environment
1	1/8-th scale	Impactor	No media	Lab. and flight
2	1/8-th scale	Scroll media	MERV 13 and 15	Lab. and flight
3	1/8-th scale	Impactor and Scroll media	MERV 13 and 15	Lab. and flight
4	Full scale	Impactor and Scroll	No media, just scroll housing	Lab. and flight
5	Full scale	Impactor and Scroll	MERV 11	Lab. and flight

## IV. Results

### A. Velocity flow field

To assess the quality of the flow field several velocity profiles in the entrance region and downstream of the filter elements were taken. The flow in the entrance region is required to be fairly uniform to minimize any secondary flow effect for filter testing. However, flow variation after the filter elements was expected. In fact the flow in this region can be quite complex depending on filter device and configuration. In particular, several profiles were obtained behind the collection bands of the impactor stage of the full scale prototype, facilitated by its larger cross-section, to ascertain the effects due to the hardware geometry.

Figure 5 provides velocity magnitude profiles at different axial stations along the length of the duct with the filter system configured with the impactor stage (the scroll filter stage was also in place but without any scroll media). The distances, normalized by the width of the collection bands, are reference with respect to the location of the impactor orifice plate. As is clearly seen, the velocity field evolves significantly over a relatively short distance (over 12.5 cm). The first downstream profile ( $x/w = 5.2$ ) shows how the flow accelerates through the orifice slots and then separates over the bands producing an alternating accelerated and wake flow pattern. The next downstream profile has a very pronounced velocity deficit above the centerline. Slightly further downstream the velocity profile is fairly flat although at an elevated velocity of 1.2 m/s. At the most downstream position, on the conic section of the filter, the profile is again flat but the mean velocity magnitude has dropped significantly to values slightly above the upstream velocity.

To investigate the spatial non-uniformity of the flow right after the impactor bands, Figure 6 shows the flow variation in velocity profiles along the horizontal and vertical direction at  $x/w = 5.2$ . These were single profiles taken at one position from the top and one from the side wall. A major velocity depression region exists to the right of the cross section and concentrated in the top half. Note that the two profiles intercept a small distance from the centerline of the duct. The velocity depression region was more than likely a product of the wake flow behind the impactor stage wiper blade which extends the all along the right wall and about 5 cm into the flow area.

The large velocity depression found behind the impactor collection bands can affect the performance of downstream filter elements. The flow non-uniformity reduces the performance of the filter because the accessible filter area is reduced and flow velocities vary across the surface of the medium. However these effects seem to be sufficiently attenuated by the time the flow reaches the scroll media filter section. As shown in Figure 5, at a distance past 12 impactor band widths the flow has recovered to a mostly flat or uniform velocity front, which coincides with the leading pleats of the scroll media filter. Since the complex flow likely originates from the wake flow from the impactor wiper, one remedy in the next generation prototype will be to place the wiper blade as well as the belt pulleys as much as possible outside the flow path.

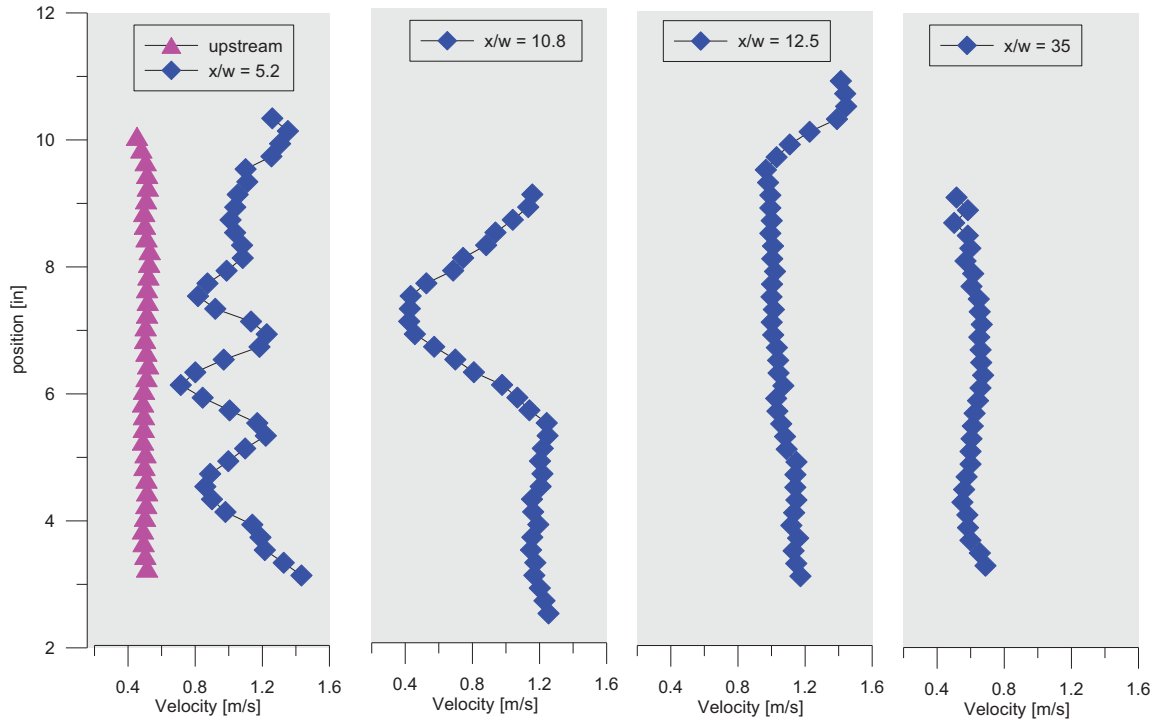
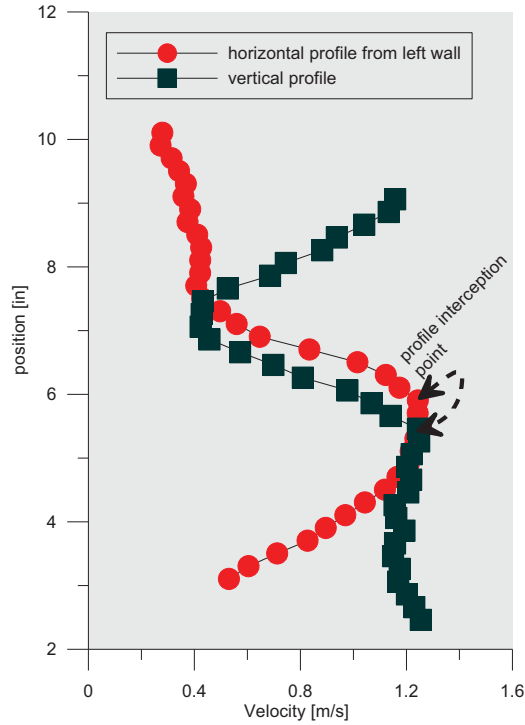


Figure 5: Velocity Magnitude profiles at different vertical axial stations



**Figure 6: Vertical and horizontal profiles at  $x/w = 5.2$**

Light sheet imaging was also used a diagnostic tool to characterize the upstream flow and associated particle transport. The picture in Figure 7 clearly shows a particle cloud emanating from the particle generator (left). The image also shows that the particle cloud spreads quickly after leaving the particle generator. While there are flow structures visible in the particle cloud, these structures are expected to disperse and dissipate sufficiently by the time it reaches the sampling probe and the first filter element (not confirmed by data). The metallic structure on the right is the inlet of the sampling probe used to measure the upstream particle counts.



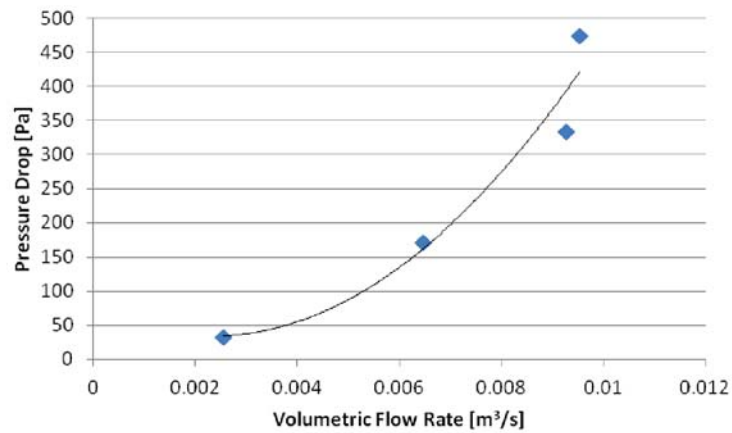
**Figure 7: Laser sheet image of upstream particle flow.**

Permeability of the filter elements was one of the initial performance parameters measured. Based on the definition of permeability given previously, the higher the permeability the greater the flow capacity through the filter. The permeability of the two different scale filter samples tested, presented in Table 2, seem to stay about the same indicating that scaling of the filter geometry did not change the performance of the filter medium. A slightly larger permeability was produced the lower grade MERV filter as expected. Permeability was not expected to change with gravity levels.

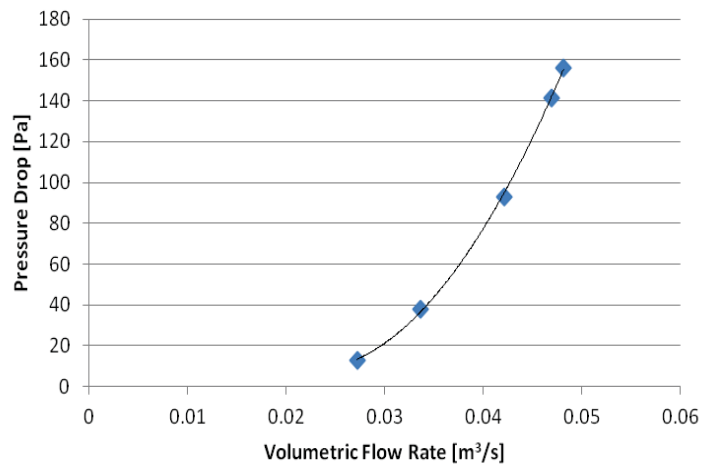
**Table 2: Filter media permeability**

Filter type	Permeability @ 100 Pa [m <sup>3</sup> vol. flow/m <sup>2</sup> area/s]
Full Scale Scroll media (MERV 11)	0.65
1/8th scale scroll media (MERV 13)	0.59

In Figure 8 the pressure drop across the impactor stages of the two prototypes at various velocities at laboratory ambient conditions is presented. There is clear distinction between the scaled and full scale prototype in the magnitude of pressure drop. There seems to be significant differences in the slopes of the two curves, with distinctly steeper slopes attributed to the scaled prototype (note that due to the large difference in nominal flow rates of the two prototypes their respective curves could not be plotted on the same basis scale). This most likely is due to the design of the orifice plate on the scale prototype which consists of several hundred 1 mm diameter size holes in front of each band, as compared to the larger slots on the full scale prototype. As is seen in both cases, but more particularly with the scaled prototype, the pressure drop rises rather significantly with small changes in face velocities. At about 0.52 m/s on the full scale prototype the pressure drop has reached 125 Pa or 0.5 inches of water, and 150 Pa for the scaled prototype. Based on these curves, it seems there is an advantage hydrodynamically to using the more open design of the full scale prototype.



(a)



(b)

**Figure 8: Impactor stage performance curves (a) scaled prototype, (b) full scale prototype**

### B. Filtration testing

One effect of the low-g and zero-g environment is a lower, and absence of, particle settling respectively of all particle sizes. Since settling velocity scales with the square of the particle diameter, then the effect increases significantly with particle size. If however gravity is reduced or eliminated the population of larger particles should increase in relation to the total particle population. Therefore the distribution of suspended particles entrained in the flow should start to shift upward in the upper particle range. Figure 9 shows the upstream population distribution of particle sizes under different gravity levels obtained from the flight data. At 1-g the distribution is shifted towards the lower particle range. There is a shift in the peak value (except for the Martian case) to the right for all other gravity levels accompanied with an increase in population of the largest particle sizes as predicted.

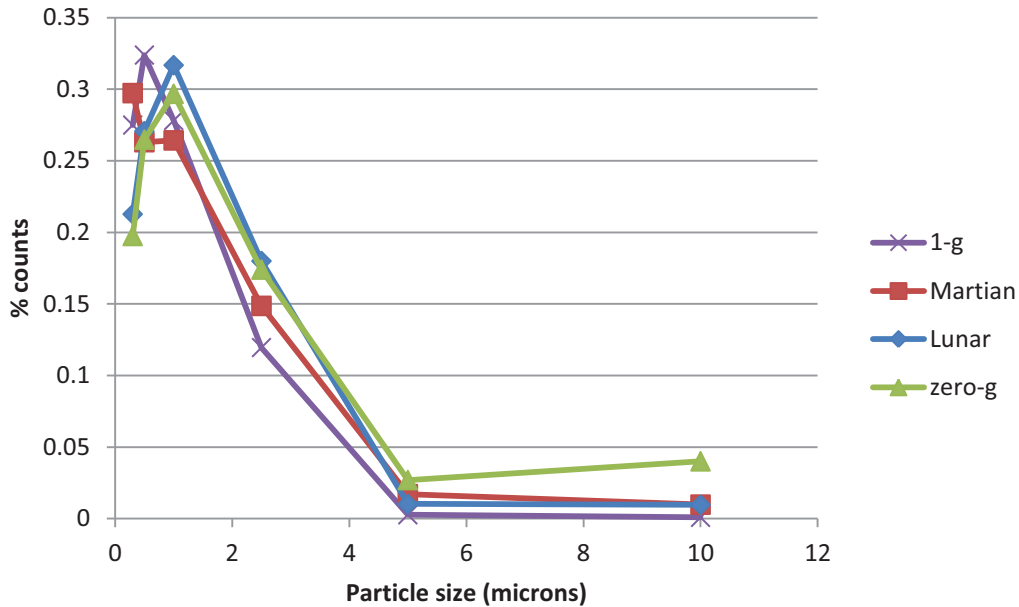


Figure 9: Particle size distribution in the upstream flow.

Particle penetration, or capturing efficiency, performance was obtained for the impactor filter stage and the combined impactor and scroll filter stages. First a note of caution should be highlighted here in light of the discussion in the previous section regarding the flow complexity after the impactor stage. We are using testing methods designed for media filters, in which flow patterns are expected to be steady and remain fairly rectilinear. The flow unsteadiness can be accounted through statistical sampling over sufficiently long times, while to account for the flow divergence, or curvilinear motion, one must assume that there are direct streampaths between the upstream and downstream sampling probe. The collection efficiency is presented here with these caveats. In addition, the laboratory data was considered statistically more significant than the flight data because of the greater number of tests that were performed. Another aspect of the low-g measurement is that operations during the flight were challenged by variations in low-g levels and the transition from high-g to low-g levels that affected the transport of the solid particles as they left the particle generator. Lastly, the shorter distance between the particle generation source and the upstream particle sampling probe in the scale prototype most likely produced more conservative upstream particle count numbers, and thereby skewed the capturing efficiency calculations. Therefore, the results presented in this section are focused mostly on the collection efficiency data of the full scale prototype, with some comparison to the data from the scaled prototype.

The operation of particle generator during ground tests went smoothly. Figure 10 gives the efficiency data for the impactor stage alone. The laboratory data sets at the two different flow speeds tend to follow each other closely, showing generally high capturing efficiency with local drops in efficiency at particle sizes of 0.3  $\mu\text{m}$  and 5  $\mu\text{m}$ . The drop in efficiency at 0.3  $\mu\text{m}$  is consistent with media filtration theory as discussed in section II.A. The reason for the drop at 5  $\mu\text{m}$  is not fully understood. It may have something to do with a change in sensitivity in signal detection at this size channel between the two particle counters. Particle bounce and re-entrainment of larger particles, a phenomenon noted in commercial testing, may also be at play. The low-g data is significantly different at the smallest particle sizes up to 2.5  $\mu\text{m}$ , while at the largest particle sizes it agrees with the laboratory data. It is not clear what the low efficiencies in the smallest particle range is attributed to. One possible cause could be g-jitter from the plane which causes particles to skip around in the flow due to inertial effects. However, this does not explain why the largest particle sizes, which should be the most susceptible to these effects, are not also affected. The more plausible reason could be that there is additional flow unsteadiness in the low-g case which causes the particle flows, particularly the smallest particles, to become more randomized in the flow. The larger standard error, from multiple repeat test runs, in the low-g data is an indication of this possibility.

The capturing efficiency for the two combined stages, impactor and scroll filter, is given in Figure 11. Because of a lack of a media tensioning mechanism, there was some slack in the media that tended to bow out the media between the spindles used to form the pleats from the flow pressure. The filter system was tested under these

conditions, although manual tensioning was applied on later tests. The plots show that there is generally better agreement between the laboratory and low-g data down to the 1  $\mu\text{m}$  size range, with efficiencies greater than 90%. Also there is small rate of efficiency roll-off towards the smallest particle sizes in all cases in the graph, which is more pronounced for the low-g data.

After a series of tests that loaded the filter medium and collection surfaces with an accumulation of particles, the impactor stage bands were cycled half way around and the scroll media was rolled up on the collection spool exposing the flow to fresh new media. Pictures of the loaded impactor stage bands are shown in Figure 12. The particle deposits show up as streaks on the full scale prototype because of the use of orifice slots, while distinct circular spot deposits are visible in the loaded impactor bands of the scale prototype produced by the arrays of millimeter diameter orifice holes. The scrolling operation was activated by switching on the servo motor. The operation went smoothly throughout the whole process, where the loaded media rolled up tightly and orderly on the collection spool. The power draw on the servo motor was 7.2 Watts at a rotation rate of 0.26 revolutions per second. The final efficiency curve given in Figure 13 shows a comparison of efficiencies before and after the scrolling of the media. The two plots generally agree well. For these two cases, the media was manually tensioned using a hand crank at the supply spool to mitigate the media bowing effect. The similar high efficiencies before and after scrolling of the media show there was no adverse effect produced by the self-cleaning operation of scrolling the media.

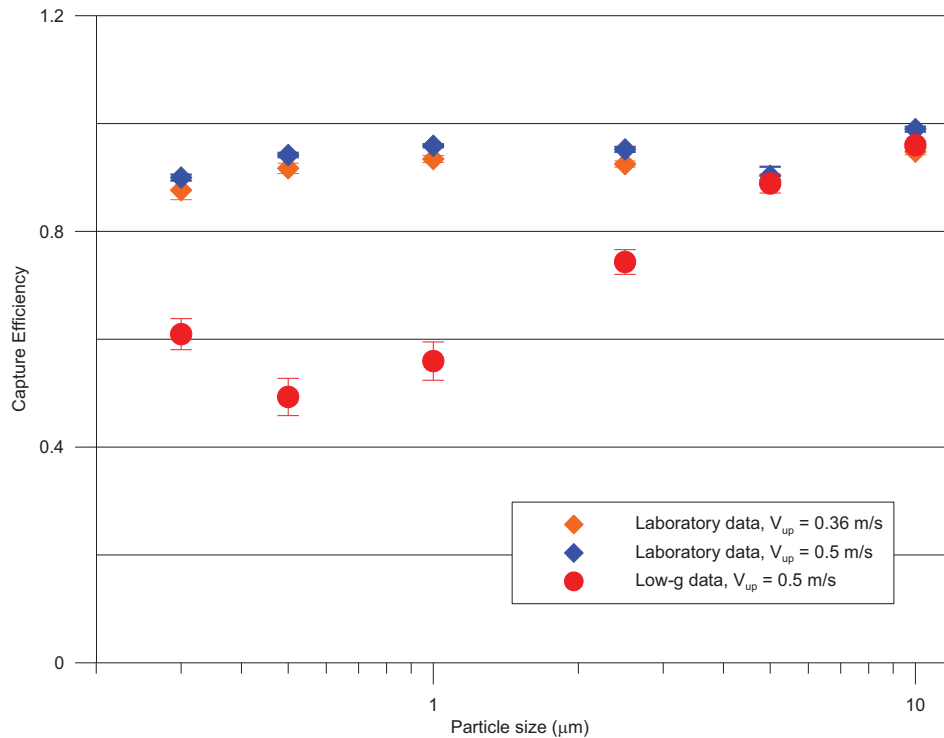


Figure 10: Particle Collection Efficiency of Impactor Stage.

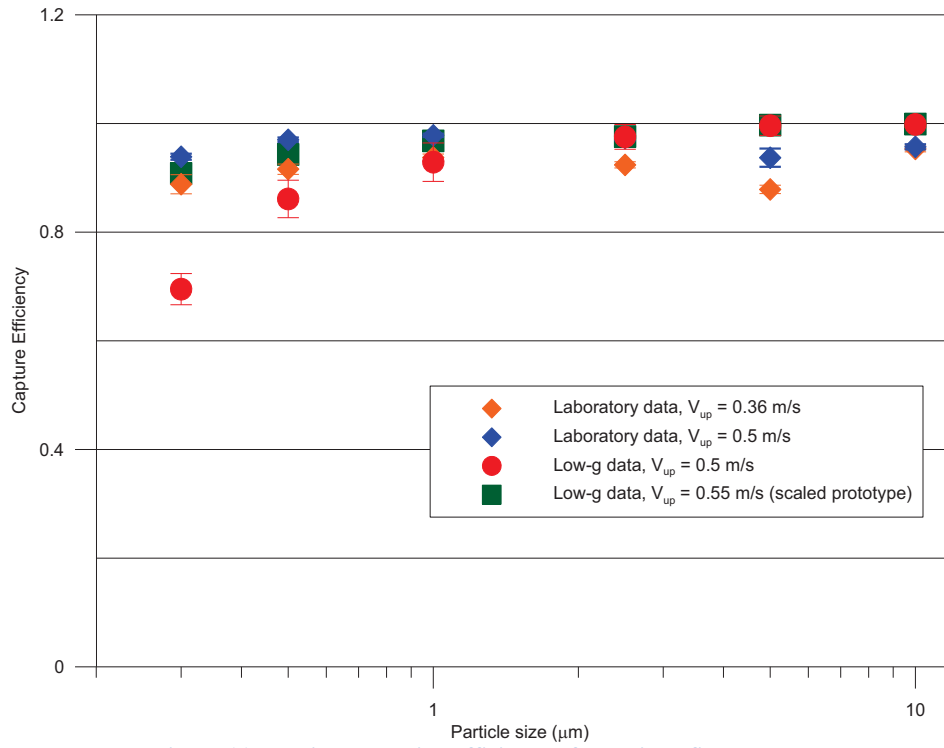


Figure 11: Particle collection efficiency of combined filter system.

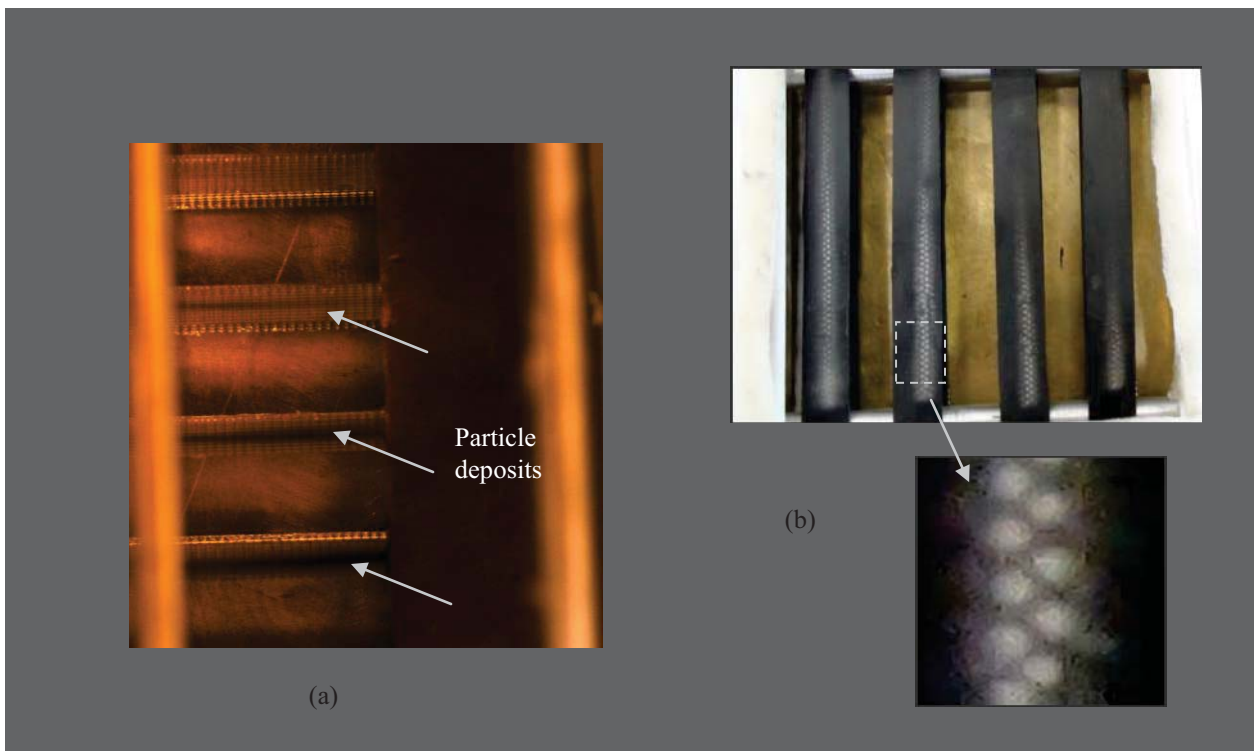


Figure 12: Particle collection efficiency of combined filtration system before and after regeneration.

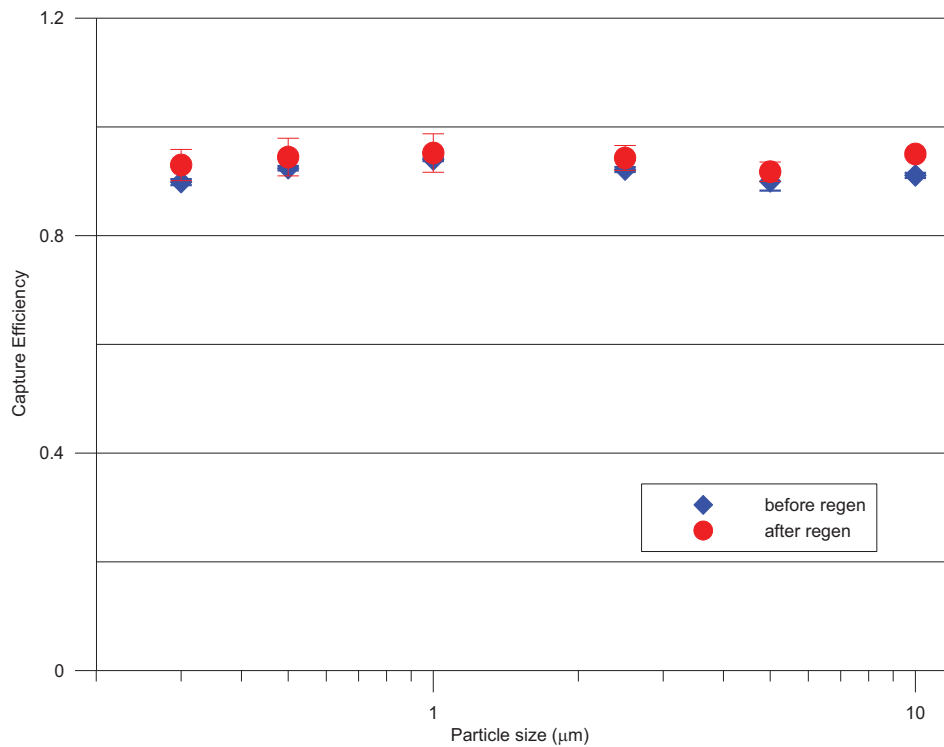


Figure 13: Picture of impactor collection bands after regeneration. (a) Full scale prototype, (b) scale prototype.

## VI. Conclusion

A novel air filtration system for crewed vehicles and extraterrestrial outposts has been developed through a partnership between NASA and Aerfil. The filter system consists of several stages of filtration including an inertial impaction stage, an indexing (or scroll) media stage, and a final high efficiency filter media stage. An 1/8-th scale and full scale prototype of the filter system were constructed and subsequently tested at NASA GRC under laboratory ambient conditions and on the Zero-G Corp aircraft in low gravity. The tests demonstrated the filter system provided good overall performance. Particle collection efficiencies greater 90% were found for the system as a whole with the combined stages. Regeneration was also shown to perform satisfactorily at relatively low power. There was general agreement between the ground and laboratory tests, but discrepancies were found at the smallest particle sizes possibly due to flow unsteadiness. Additional testing at low-g conditions may be required to resolve this. Areas of improvement were identified through testing the filter system. These included better sealing, relocation of wiper, and provision for tensioning the scroll media.

## Acknowledgements

We will like to acknowledge several individuals for their valuable support and assistance in this development. We thank Mr. Vinay Bothra of Spectrum Filtration for his company's fabrication support of the full scale prototype; Dr. Marcos Aldoph of Trox do Brasil for providing the HEPA filters used in testing; Dr. Jeff Mackey of Vantage Partners LLC for his role in setting up the flight rig; Mr. Mark Hyatt of NASA GRC for his very supportive project manager role; and Larry Ost of Filtration Group Incorporated for his role in the fabrication of the scale prototype. We also thank all those involved in the various flight campaigns providing ground support and participating in flight operations: Mr. Vinay Bothra, Dr. Marcos Aldoph, Dr. Vinod Vijayakumar (Aerfil), Dr. Jeffrey Mackey, Mr. Mark Hyatt, and Mr. Logan Larson (University of Michigan).

## References

<sup>1</sup> Hinds, W.C. *Aerosol Technology: Properties, Behavior, and Measurement of Airborne Particulates*, 2<sup>nd</sup> Ed., Wiley-Interscience, New York, 1999, Ch. 5.

<sup>2</sup> “In Situ Solid Particle Generator.” NASA Tech Briefs, Jan. 2013 issue (vol. 37, no. 1)

<sup>3</sup> American Society of Heating, Refrigeration and Air-Conditioning Engineers (2007) “Method of Testing General Ventilation Air-Cleaning Devices for Removal Efficiency by Particle Size,” ASHRAE 52.2-2007

<sup>4</sup> Institute of Environmental Sciences and Technology (2007) “HEPA and ULPA Filters,” IEST-RP-CC001.5

<sup>5</sup> International Organization for Standardization (2011) “High-efficiency filters and filter media for removing particles in air -- Part 2: Aerosol production, measuring equipment and particle-counting statistics,” ISO 29463-2.

<sup>6</sup> Orbitec Corp. (2006) “CHARACTERIZATION SUMMARY OF JSC-1AF LUNAR MARE REGOLITH SIMULANT,” URL: [http://www.orbitec.com/store/JSC-1AF\\_Characterization.pdf](http://www.orbitec.com/store/JSC-1AF_Characterization.pdf).